Charge transfer excitons in polymer/fullerene blends: the role of morphology and polymer chain conformation

By *Markus Hallermann*, *Ilka Kriegel, Enrico Da Como*,* *Josef M. Berger, Elizabeth von Hauff* and *Jochen Feldmann*

[*] Dr. E. Da Como, M. Hallermann, I. Kriegel, J. M. Berger, Prof. J. Feldmann
Photonics and Optoelectronics Group, Department of Physics and CeNS
Ludwig-Maximilians-Universität, 80799, Munich (Germany)
E-mail: enrico.dacomo@physik.uni-muenchen.de

Dr. E. von Hauff
Institute of Physics, Energy and Semiconductor Research Laboratory
Carl von Ossietzky University, 26111, Oldenburg (Germany)

[**] We thank S. Niedermaier and A. Helfrich for technical assistance. We are grateful to the DFG for financial support through the SPP 1355 "Fundamental processes in organic photovoltaics" and the BMBF through "OPV-stabilität". The German Excellence Initiative is also acknowledged for funding via the "Nanosystems Initiative Munich (NIM)".

Keywords: (conjugated polymers, fullerenes, morphology, recombination, organic photovoltaics)

Abstract

We show how carrier recombination through charge transfer excitons between conjugated polymers and fullerene molecules is mainly controlled by the intrachain conformation of the polymer, and to a limited extent by the mesoscopic morphology of the blend. This experimental result is obtained by combining near infrared photoluminescence spectroscopy and transmission electron microscopy, which are sensitive to charge transfer exciton emission and morphology, respectively. The photoluminescence intensity of the charge transfer exciton is correlated to the degree of intrachain order of the polymer, highlighting an important aspect for understanding and limiting carrier recombination in organic photovoltaics.

1. Introduction

Heterojunctions are starting to be ubiquitous in organic optoelectronics. In organic light emitting diodes heterostructures are used to effectively confine charge carriers or excitons to a specific emitting layer, thus enhancing the electroluminescence efficiency.[1, 2] In photovoltaic cells heterojunctions are at the basis of operation, in order to obtain photo-induced charge transfer (CT), i.e. the crucial step for energy conversion.[3, 4] Several studies have highlighted the advantages of conjugated polymers/fullerene heterojunctions as ideal material systems to harvest the visible part of the solar spectrum and convert energy into electrons and holes after exciton dissociation.[4-6] The working principle is based on the light absorption by conjugated polymer chromophores, charge separation at the interface with the fullerene and charge carrier collection in the presence of the open circuit voltage of the cell. For this type of solar cells it was soon recognized that the limited exciton diffusion length (~10 nm) characterizing most conjugated polymers,[7, 8] requires interpenetrating networks with the fullerene acceptor molecules, enabling a larger probability for CT instead of exciton recombination in the polymer. These blends are commonly termed bulk heterojunctions and consist of intermixed nanoscale domains of the two components, owing to the phase separation occurring between the two materials. As an additional feature, such morphology provides preferential percolation paths for electrons and holes in the fullerene and polymer domains, respectively. While the electronic structure of the pristine materials has been well characterized, little is known about the interface states in the blends, though they are necessarily participating to the CT process.[9, 10] The abundance of these states is expected to be influenced by the blend morphology as they are bound to the interfacial area of the heterojunction. This is also envisaged by the substantial progress made in optimizing the mesoscopic morphology in correlation to the solar cell efficiency.[6, 11, 12] While control over morphology is known to improve charge carrier mobility, it is not clear a priori what is the effect on carrier recombination,[6] one of the major

limits in advancing organic solar cell technology.[13, 14] Unfortunately, a clear identification of the molecular parameters governing recombination through interface states is still elusive and experimentally challenging.

CT states are a result of interfacial electronic interactions occurring at the heterojunction between organic semiconductors.[15-17] These states can be considered as *hybrid states* originating from the wavefunction overlap between an acceptor and a donor molecule in close contact.[18-22] The overlap can involve both highest occupied molecular orbitals (HOMOs) and lowest unoccupied molecular orbitals (LUMOs), resulting in the formation of hybrid ground[9, 17, 19, 23-25] and excited states,[26-29] within the optical gap of the two materials. When considering excited states these are generally named charge transfer excitons (CTE), or exciplexes in the case of relaxation to unbound ground state.[30] So far it has been proposed that electronic interactions through charge transfer states have a beneficial role in some polyfluorene based solar cells.[17, 29] In particular, an influence on charge separation was invoked as a positive effect in the above cited works. In contrast to these reports, recent investigations demonstrate how charge transfer states could be a limiting factor for maximizing the open circuit voltage of the cell,[31, 32] one of the key parameters affecting the efficiency, together with short circuit current. The latter parameter is controlled by the charge carrier mobility in the two materials and limited by recombination of the photogenerated charge carriers. We infer that CT states should have also a role in the short circuit current of the cell, for instance leading to a facilitated electron and hole recombination through CTE photoluminescence (PL). It is important here to distinguish between *geminate* and *non-geminate* recombination. The first occurs within the first few nanoseconds after photoinduced CT, the latter involves separated charge carriers that recombine in the micro- and millisecond time scale after carrier diffusion in the respective domains. In light of CT states participation in the crucial steps for photovoltaic action, it is imperative to understand the molecular

characteristics which control their formation and the effect of the mesoscopic morphology. This remained so far an intriguing issue, primarily because of the experimental difficulties in observing and characterizing CTEs. As a consequence studies attempting to address the role of morphology and molecular structure on CTE formation are rare, necessitating the combination of optical spectroscopy with high resolution microscopy for material systems with well defined modifications in the chemical structure. Such modifications, when applied to the conjugated polymer, can be very important to test the role of chain conformation in CTE.

Here, we show that CTE PL can be observed in efficient polymer/fullerene combinations such as poly[2-methoxy-5-(3`,7´-dimethyloctyloxy-1,4-phenylene-vinylene] (MDMO-PPV) and regioregular poly[3-hexylthiophene] (RE-P3HT) when blended with 1-(3-methoxycarbonyl)-propyl-1-phenyl-(6,6) C_{61} (PCBM) (see Fig.1b for chemical structures). We based our results on near-infrared (NIR) sensitive PL spectroscopy. Moreover, by covering the visible spectral range, these experiments offer the possibility not only to monitor recombination from the CTE, but also from the fullerene and polymer excited states, providing a thorough picture of radiative recombination in polymeric solar cells. CTE PL is likely to be a geminate recombination process. To correlate the presence of CTE emission with the interfacial area between the polymer and the fullerene, we have performed transmission electron microscopy (TEM) on the same blends. We first consider the PL emission of MDMO-PPV/PCBM blends, focusing on CTE emission and correlate it with the interfacial area between domains of the two materials varied by changing the components weight ratio. Recombination in the form of CTE emission is present as a prominent PL band without a strong dependence on morphology and weight ratios. The P3HT/PCBM blends considered in a second series of experiments allows for distinguishing between the effect of morphology and chain conformation. The latter effect has been tested by comparing RE-P3HT with regiorandom P3HT (P3HT), i.e.

polymers with the same chemical structure in the backbone, but different chain conformations due to the side groups. Interestingly, we observe that the CTE emission is influenced by the intrachain conformation of the polymer, rather than by morphology. The results demonstrate how by changing the intrachain characteristics of the polymer, it is possible to limit the recombination through CTE.

2. Results and Discussion

The left panel of figure 1a illustrates the three main recombination processes (straight arrows) after light absorption in a polymer/fullerene blend. In this excitonic energy scheme the singlet exciton levels of the conjugated polymer and the fullerene (S_1) are located at higher energy with respect to the CTE.[9] The spectrum on the right hand side provides a snapshot of the potential of visible/NIR PL spectroscopy in resolving carrier recombination in different sites making up the bulk heterojunction, in this example MDMO-PPV/PCBM. The dashed lines assign the emission peaks to the respective electronic states as detailed below. Triplet excited states are not considered in this scheme, since they are known to be at higher energy with respect to the CTE.[32, 33] For other material combinations, where the triplet excitonic level of the donor or acceptor is below the CTE, these are known to play an important role in recombination.[33, 34] Figure 2a-d shows the visible/NIR PL spectra of four MDMO-PPV/PCBM thin films, characterized by different weight ratios of PCBM (20%, 40%, 60% and 80%, respectively). In the spectra of Fig. 2a, b two main transitions are apparent; the singlet exciton in MDMO-PPV (2.19 eV) and a red shifted broad emission peaking at 1.35 eV and extending to the NIR down to 0.9 eV. This second feature is assigned to charge carrier recombination from the CTE formed at the polymer/fullerene molecular interface. Such interpretation is supported by our recent measurements on electric field induced quenching of CTE emission.[28] In agreement with reports dealing with CTE in other blends, this emission is quenched at relatively low field with respect to the S_1 exciton as a consequence of the

reduced Coulomb interaction between the hole on the donor and electron on the acceptor.[27, 28] Since in our experiment light is primarily absorbed by the polymer (excitation at 520 nm), CTE are populated by photoinduced electron transfer from MDMO-PPV to PCBM. Therefore, the CTE PL band can be used as a sensitive spectroscopic signal to monitor primarily geminate recombination at the heterojunction after the initial charge transfer. Fig. 2c reports the results from the same type of experiment performed on a blend with 60% PCBM. In this case a third PL transition appears at 1.7 eV. The inset of this figure shows the reference PL spectra of thin films obtained from the pure materials and the peak at 1.7 eV is assigned to the PL from PCBM (thick line in the inset).[35] Here, it is important to note that the intensity of the PL originating from S_1 excitons in the MDMO-PPV and PCBM are not only dependent on the amount of the respective component in the blend film, but also on the probability of the exciton to be quenched. Quenching essentially depends on exciton diffusion to the common interface and charge transfer. By increasing further the PCBM weight ratio (80% panel d), we note a more intense and resolved PCBM emission, consistent with more fullerene molecules present in the sample, but also with a morphology which promotes recombination in the PCBM domains, instead of diffusion to the interface (see below).

We have complemented these spectroscopic fingerprints with TEM images of the films (Fig. 2e-h). TEM has proven to be a powerful tool for studies on morphology in polymer/fullerene bulk heterojunction solar cells.[36, 37] As a consequence of differences in the electron density between fullerenes and conjugated polymers, it is widely recognized that darker regions correspond to fullerene rich domains.[27, 35, 37, 38] For the 20% sample (Fig. 2e) a bright contrast dominates the image with a few dark spots. This demonstrates the presence of a continuous film of MDMO-PPV as the major constituent, in the presence of a few PCBM regions. For higher PCBM concentrations (panel f-h), the PCBM domains appear as circularly shaped regions, that span diameter sizes from 30 to 200 nm. We do not exclude the presence of

MDMO-PPV also in the dark domains (and vice versa), as discussed in previous investigations on morphology.[35, 39] In the 80%, the very high concentration of fullerene derivative results in the coalescence of the dark domains. Correspondingly, regions rich in MDMO-PPV have now reached small sizes of the order of a few tenths of nanometers.

We now focus on the comparison between the TEM pictures and the corresponding PL spectra looking primarily at CTE emission. To effectively quantify the intensity of the different bands and facilitate our discussion, we have plotted in Figure 3 the integrated PL intensity of the transitions as a function of MDMO-PPV/PCBM weight ratio (wt %). For completeness a 0% sample (pure polymer) has been included (not shown in Fig.2). Upon addition of the fullerene the MDMO-PPV PL (empty squares in Fig.3) is quenched by an order of magnitude, in accordance with previous studies[39] (note the break in the PL intensity scale). The decrease in intensity of MDMO-PPV PL, when increasing PCBM content from 20% to 40%, is a consequence of more effective exciton dissociation. This behaviour is correlated with the decreasing trend in domain size of the polymer as seen in the corresponding TEM pictures (Fig.2e,f). Indeed, when the domain size approaches dimensions comparable to the singlet exciton diffusion length of PPV-based polymers (~20 nm),[40] a larger number of excitons reaches the interface and charge transfer occurs. Therefore, as expected the fluorescent emission of MDMO-PPV is much more efficiently quenched in blends with small polymer domains (60% and 80%) than large ones (20% and 40%). An increasing amount of PCBM molecules (Fig. 2g and 2h) results in the appearance of the transition at 1.7 eV, which is the result of exciton recombination in PCBM. Similar to the case discussed for the polymer excitons, emission from PCBM is influenced by domains size and the exciton diffusion length. This is clearly demonstrated by observing an increase in intensity when going from 60% to 80% (black dots in Fig.3). In the 80% sample a larger quantity of

excitons in PCBM can recombine without reaching the interface with the polymer, where hole transfer occurs.[41]

Remarkably, all the PL spectra of the blends in Fig. 2 show a CTE PL band. According to Fig. 3 the intensity of the CTE transition (diamonds) has a maximum intensity at 20% and is constant for weight ratios larger than 40%. As discussed above, such emission should originate exclusively from the interfacial area between the two materials. We have performed a quantitative analysis of the TEM images by counting the number of pixels at the interface between fullerene and polymer domains and normalizing it to the total number of pixels in the image. Such analysis was performed by considering a total of 80 TEM pictures taken at different positions in the three films at 20%, 60% and 80% weight ratio (see experimental part for details). The relative abundance of interfaces with the increasing weight ratio of PCBM in the samples of Fig.2e,g,h is (4 ± 1.7)%, (21 ± 3.3)% and (10 ± 3.2)%, respectively. Therefore, as apparent in Fig. 2g at 60% PCBM there is more interfacial area between domains. Considering this analysis the most intense CTE emission should be recorded for the 60 % sample and not for the 20% as the optical experiments indicate. The high intensity of the CTE in the 20% sample is surprising and does not correlate with the low (4%) abundance of interfaces (Fig.2e). To explain this result we assume the presence of *molecularly dispersed* PCBM in films with a PCBM content <40%, which is not evident in the TEM images at such a resolution. These isolated molecules are likely to be preferential CTE recombination centres, which do not contribute to photocurrent when present in devices. From a morphological point of view, we can consider this observation as a proof for incomplete phase segregation, i.e. the domains observed in TEM are not always pure, but more likely rich in one of the two materials. Above 40% PCBM content, we infer that phase segregation has started to occur in accordance with previous reports.[35, 42] Beyond 40% the CTE intensity appears to be rather insensitive to changes in the interfacial area and is likely to be a more

intrinsic characteristic, probably due to the molecular properties of these two materials rather than being controlled by changes in interface area (morphology). Summarizing the results for MDMO-PPV/PCBM, we have attempted to correlate the morphology and the charge carrier recombination occurring in the domains of the components and at the interface. NIR PL spectroscopy can provide unique information on CTE emission, which has been observed for all the different concentrations with a weak dependence on morphology. Therefore, it appears to be an intrinsic characteristic of MDMO-PPV when mixed with the fullerene acceptor PCBM, probably linked to the chain or chromophore conformation of MDMO-PPV at the interface with fullerene.

A material combination which is suitable to test effects of the polymer chain conformation is P3HT/PCBM. Indeed, P3HT offers the possibility to have changes in the polymer conformation by having the hexyl side-groups in a regio-random (ra-P3HT) or regio-regular arrangement (RE-P3HT). Besides this important possibility, RE-P3HT shows photovoltaic efficiencies of up to 5% when blended with PCBM at about 50% weight ratio[43] (see Fig. 1b for chemical structures). This makes it an even more interesting material combination for solar cells compared to MDMO-PPV/PCBM, where efficiencies of about 2.5% were reported.[11] The high hole mobilities observed in RE-P3HT have been considered to be one of the reasons for better performances.[6] In RE-P3HT/PCBM blends it is however crucial to control the interchain order in the polymer domains, to achieve crystalline regions (lamellae). The lamellae structure leads to increased carrier mobility as discussed in several reports.[44, 45] While it is known that the *intrachain order* provided by the regioregularity is a necessary condition for lamellae formation, it has not been addressed if the order has an effect on CTE formation and therefore on recombination. CTE emission in polythiophene/fullerene combinations remained elusive so far.[33] With the idea of probing the effect of polymer chain conformation, we have first attempted to observe CTE in the visible/NIR PL spectrum of ra-

P3HT/PCBM, where intrachain order is disrupted by the randomness of the side group position on the thiophene ring. The normalized spectrum of the blend (50% wt ratio), thick solid line in Fig.4a, shows a modified PL emission from the S_1 exciton with respect to the pristine polymer (thin line), peaking around 2.0 eV. The shift of the S_1 emission to higher energies might be due to a change in the conformation of the polymer chromophores in the blend. The most important feature is the additional prominent emission at 1.2 eV in the blend. Very similarly to what is observed above for MDMO-PPV/PCBM, we assign this emission, appearing exclusively in the blend, to the CTE between ra-P3HT and the fullerene. The difference in the energetic position with respect to the MDMO-PPV/PCBM CTE can be nicely traced back to a change of ~0.1 eV in the HOMO position between the two polymers (see table 1 in Ref. [46]). In Fig. 4d we report the intensity of the different transitions as a function of the PCBM concentration, in a similar way to Fig.3 for MDMO-PPV based blends. The trend is very similar to what is observed for the above described blend, with a quenching of more than an order of magnitude upon blending. It is also important to note the small variations in the CTE emission above 50%, suggesting a little effect of PCBM weight ratio like in MDMO-PPV/PCBM.

If we now consider the same polymer backbone with an ordered intrachain conformation such as RE-P3HT (thin solid line in Fig.4b), we note almost no differences in the spectral shape upon PCBM blending (thick solid line), i.e. no additional transitions seem to appear in the spectrum. Differences become evident only when enlarging the scale on the red tail of the spectrum, in which the intensity was multiplied by a factor of ten. Here, we distinguish a shoulder at about 1.2 eV only present in the blend film, which we assign to the CTE in RE-P3HT/PCBM. The most striking result for this blend is the relatively low intensity of CTE PL, when compared to the results for MDMO-PPV/PCBM (Fig.2) and ra-P3HT/PCBM (Fig.4a). Such a low intensity does not allow us to perform any quantitative analysis on CTE

intensity, as carried out for the other blends. We report in Fig. 4e only the quenching of the polymer PL upon blending the PCBM. The trend indicates efficient photoinduced charge transfer as confirmed in studies combining quenching of PL and transient absorption spectroscopy.[33] The observation of a very weak CTE emission is symptomatic of a reduced recombination through CTE and correlates with the large short circuit currents and efficiencies reported for such a material combination. By looking at the morphologies of the two P3HT/PCBM blends introduced so far (Fig. 4f and 4g), we observe different structures, but with an equally abundant amount of interfaces (24% for RE-P3HT and 21% for ra-P3HT) between the two materials. Interestingly, the CTE emission, which is assumed to depend on the interface area, is changing by almost an order of magnitude apparently only as a function of chain conformation. To gain insights about the interplay between *molecular intrachain* and *mesoscopic morphological* effects on CTE emission, we have also studied annealed films and made a comparison with the mesoscopic morphology. While the annealing leads to the expected modifications in morphology (compare Fig.4g and 4h)[36], only a little difference in the CTE emission is observed (dashed line in Fig.4c). We conclude that in P3HT/PCBM the mesoscopic morphology plays a limited role in governing geminate carrier recombination through CTE excitons, this appears to be more influenced by the polymer chain conformation. Annealing of this blend remains important in creating lamellae structures necessary for high carrier mobility and preferential percolation paths.[6]

Considering all the results reported for the different material combinations, it appears that differences in CTE recombination can originate at the molecular level and only partially in the mesoscopic structure of the film. It remains however unclear, which molecular parameters are controlling the wavefunction overlap between the polymer and the fullerene and thus CTE emission. In polythiophenes small modifications in the side groups are expected to impact directly on the chain rigidity and the electronic structure. This is readily seen in the PL spectra

of the pristine material (thin line in Fig.4a), which shows a shift towards higher energy when compared to pure RE-P3HT (Fig.4b). This has been interpreted as a reduced conjugation length, due to a larger number of torsional degrees of freedom in ra-P3HT[47]. At first sight it is not straightforward how the intrachain conformation could influence the formation of hybrid intermolecular states such as CTE. The surprising and apparently complicated behaviour of P3HT can be interpreted according to recent molecular modelling results, that show how formation of a CT interaction between conjugated polymers and molecular acceptors is accompanied by a modification in the polymer chain geometry.[18] Regio-regular polythiophenes having a rigid molecular backbone have a limited number of degrees of freedom. Therefore, RE-P3HT should present a decreased tendency in achieving modifications for wavefunction overlap with spherical molecules such as PCBM. PPV based polymers or ra-P3HT are known to have a less rigid backbone, due to the large number of torsional degrees of freedom between the repeat units.[48, 49] As our results indicate this should be favourable for CTE formation due to a closer contact with PCBM. We note in addition that localized modifications in the chain conformation should influence the intrachain hole mobility,[14, 48] decreasing the probability for hole escape from the Coulomb potential of the electron localized on the fullerene. This effect should promote recombination through the CTE. While values for the intrachain mobility of holes in P3HT and MDMO-PPV in a single conjugated unit are difficult to estimate with high accuracy, here we limit to report values for the hole mobility, $\mu_{h,}$ in blends from time of flight experiments. For RE-P3HT/PCBM blends $\mu_h = 10^{-4}$ cm^2/Vs, for MDMO-PPV/PCBM $\mu_h \sim 10^{-6}$ cm^2/Vs (ref. [6, 50]). Although these values are for thick films (> 1 μm) and consider both the intrachain and interchain hopping contributions to mobility, they are consistent with the hypothesis of a role of charge carrier mobility in CTE emission.

More in general our results suggest a clear anti-correlation between the intensity of the CTE emission measured in this work and the efficiencies reported in the literature for the same systems. For example, recent experiments by Kim et al. on P3HT/PCBM suggest that the efficiency depends on regioregularity[6]. It is worth mentioning here that preliminary NIR PL experiments performed on blends sandwiched between indium tin oxide and aluminium electrodes have shown the same intensity of the transitions as for the electrode less films. This result implies that the typical built in voltages of organic solar cells are not effective in preventing CTE recombination. We remind, however, that the photocurrent conversion efficiency involves not only the geminate recombination processes illustrated in the present paper, but also transport through percolation paths and the light harvesting characteristics of the polymer. As demonstrated in experiments based on TEM cross-sectioning, percolation paths can be effectively constructed by carefully designed processing.[51] Charge recombination and interface states remain connected to the intrachain physico-chemical properties of the polymer as our results demonstrate. Further work in the direction of chemical tailoring of intrachain order is expected to decrease further recombination losses.

3. Conclusions

We have correlated the observation of CTE in polymer/fullerene blends with morphology and polymer chain conformation. These results were obtained by the combination of NIR PL spectroscopy and TEM microscopy. For MDMO-PPV/PCBM the CTE PL intensity shows a weak dependence on the extension of interfacial area between the two materials and provides a signature for the transition from solid solutions to phase segregated blends. For this system we provide evidence for the presence of molecularly dispersed PCBM in apparently pure MDMO-PPV domains, which form preferential recombination centres. In phase segregated blends the CTE is almost independent of the film morphology, suggesting the role of polymer chain conformation in controlling the CTE emission. Such hypothesis has been verified in

P3HT/PCBM blends, where we have reported the first observation of CTE PL and shown that this emission is very sensitive to the regio-regularity of the chain side groups. Thus, the rigidity of the chain influences the wavefunction overlap between the polymer and the fullerene or the intrachain mobility modulating the CTE PL intensity. Our study provides valuable information on the influence of charge transfer states in charge recombination losses of bulk heterojunction solar cells. New strategies considering a clever design of the intrachain properties of the polymer are expected to bring improved performances by limiting CTE recombination. In addition, we stress that the NIR PL measurements presented in this work demonstrate a facile, fast and non-destructive method for estimating recombination paths in organic solar cells.

4. Experimental

Materials: MDMO-PPV, RE-P3HT, ra-P3HT and PCBM were purchased from Aldrich and used as received. RE-P3HT has a regioregularity of 98.5%. ra-P3HT has a 50% content of head to head side groups. Thin films of the pure materials and the blends were obtained by spin-coating on pre-cleaned quartz substrates in a nitrogen glove-box. The substrates were rotated at 3000 rpm for 60 s during deposition of the solutions to guarantee homogeneous films and complete solvent evaporation. Film thicknesses were in the range (380 ± 20) nm. For all the blends, solutions of the polymer and fullerene were prepared in chlorobenzene. Only spectroscopic grade solvents were used. The different weight percentages of PCBM were obtained by varying the PCBM content, while keeping the mass of polymer constant. This ensured spin coated films with comparable thicknesses. For the annealing of RE-P3HT/PCBM blends, the thin films were placed in an oven integrated in the glove box. Annealing temperatures were set to 140 °C for 10 minutes in vacuum.

For TEM measurements the floatation technique in deionized water was used to obtain free-standing films. In brief, the thin films deposited on quartz were left in the upright position

inside a Petri lab dish filled with deionized water (resistivity 18.2 MΩ*cm). After 10 minutes parts of the film, or the entire film were found floating in water completely detached from the substrate. These were collected with copper grids for TEM and dried in air. All measurements were performed on a JEOL transmission electron microscope operated at 100 kV. Image analysis was performed with the software ImageJ. The original images where subjected to Gaussian blur with a 2 nm radius and converted to black and white binary images considering the volume ratio of the components, with a similar procedure to ref. [51]. For estimating the amount of interface between the domains, the number of pixels at the interface between a white and a black domain was counted and normalized to the total number of pixels in the image.

PL spectra were obtained with a double monochromator fluorometer (Jobin-Yvon) equipped with a Peltier and a water cooled detectors sensitive in the NIR spectral range down to 0.8 eV. Measurements were performed exciting at 520 nm by a monochromated Xe-lamp, with the sample kept in vacuum at 10^{-6} mbar. No significant differences were observed for samples measured in air on a time scale of a few days.

Figures

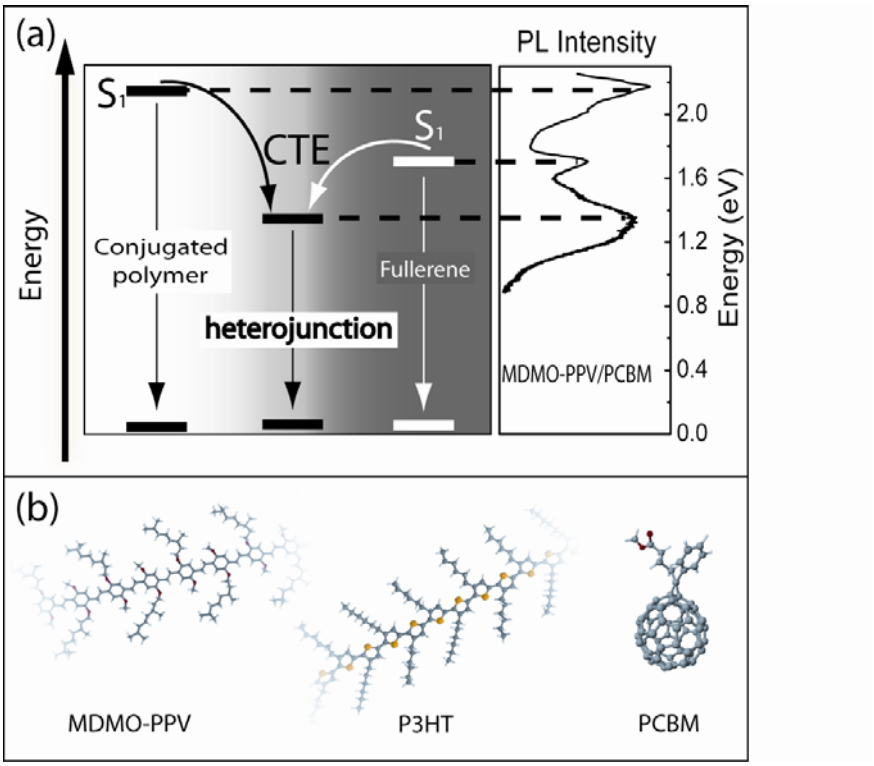

Figure 1. Schematic energy level diagram for electronic excitations in conjugated polymer/fullerene blends and PL spectrum. a) The diagram illustrates the electronic relaxation processes after light absorption by the polymer or the fullerene. S_1 indicates the respective singlet energy levels for Frenkel excitons localized on conjugated polymer chromophores or on the fullerene molecules. CTE indicates the energy level of charge transfer excitons, which are localized at the molecular heterojunction between the two materials. Straight arrows indicate relaxation to the ground state by exciton recombination and light emission in the different states. Curved arrows indicate the population of the CTE by exciton diffusion and charge transfer at the interface. The resulting PL spectrum shown on the side of the energetic scheme illustrates the possibility to monitor these transitions in a MDMO-PPV/PCBM blend. b) Chemical structures of MDMO-PPV, P3HT and PCBM.

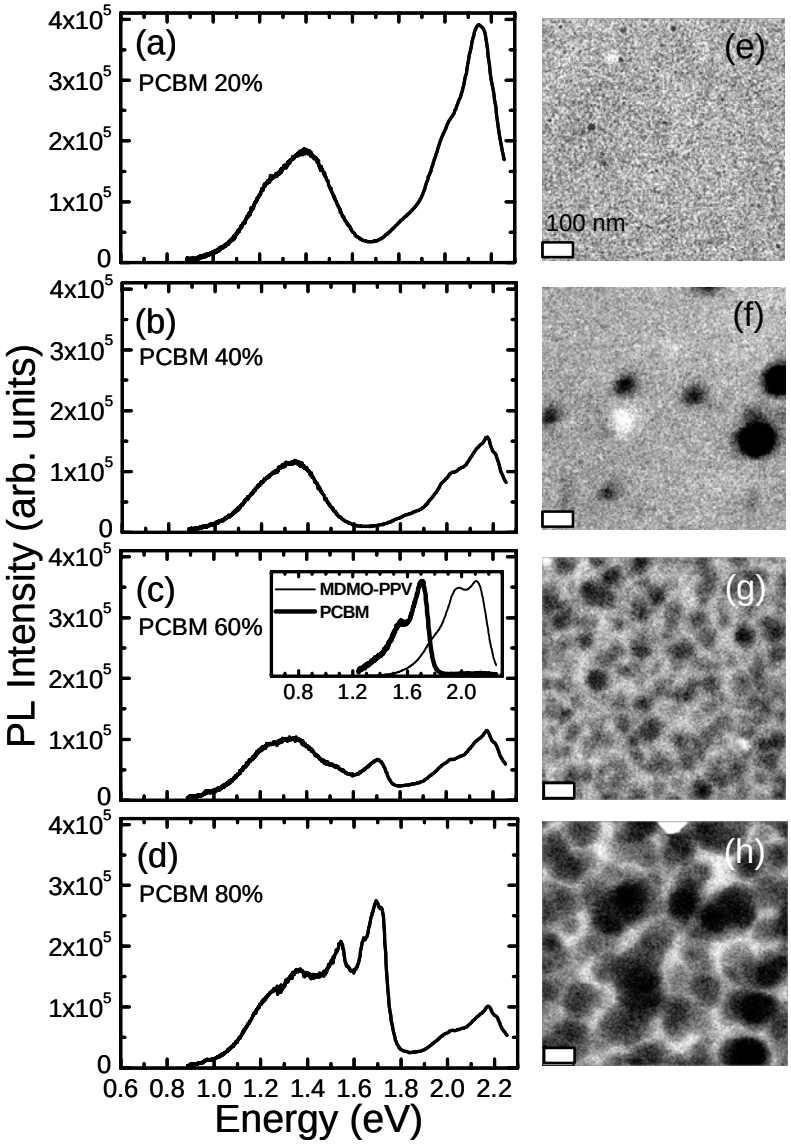

Figure 2. Correlation between PL spectra and morphology for MDMO-PPV/PCBM at different weight ratios. a) Visible/ NIR PL spectrum of a MDMO-PPV/PCBM blend film containing a 20% wt ratio of fullerene. b) ,c), d) PL spectra for samples with 40%, 60% and 80% PCBM content, respectively. The transitions at 2.19 and 1.35 eV are assigned to the MDMO-PPV exciton and CTE, respectively. The peak at 1.7 eV appearing in panel c) and d) is due to exciton recombination in the pure PCBM domains. The inset shows the PL spectra for the pristine materials: PCBM (thick line), MDMO-PPV (thin line). Excitation was performed at 520 nm and the spectra were rescaled to normalize for the amount of absorbed photons. e-h) TEM pictures obtained preparing thin films with the same weight ratio used for the optical experiments. The bright regions are representative of MDMO-PPV rich domains, while the dark ones belong to PCBM molecules. The scale bar for all the TEM images is 100 nm.

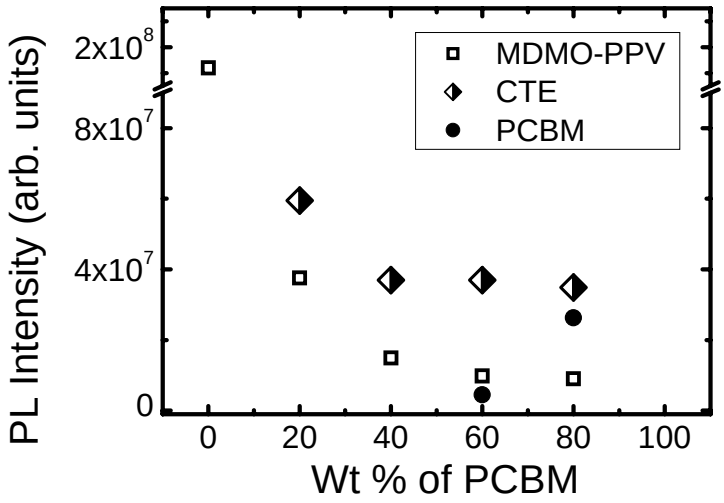

Figure 3. Influence of the blend weight ratio on carrier radiative recombination. Integrated PL intensity for the different recombination channels as a function of the PCBM weight ratio in the blends. The integrated PL of MDMO-PPV excitons is represented by empty squares, of PCBM by black dots and of CTE by diamonds.

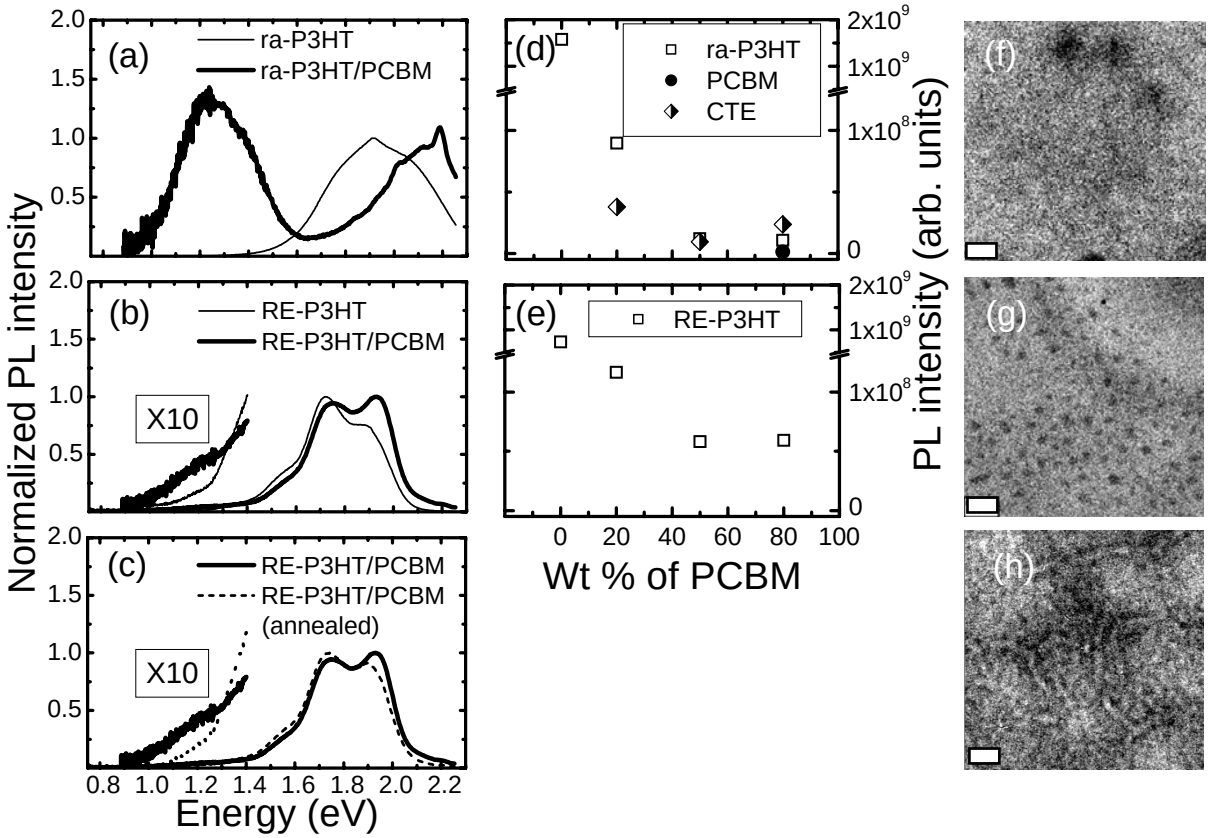

Figure 4. Interplay between morphology and intrachain regioregularity on CTE recombination in P3HT/PCBM blends. a) Visible/NIR PL spectra of pristine ra-P3HT (thin solid line) and ra-P3HT/PCBM blend film (thick solid line). b) PL spectra of pristine RE-P3HT (thin solid line) and RE-P3HT/PCBM blend film (thick solid line). c) PL spectra of RE-P3HT/PCBM (thick solid line) and the same sample annealed (thin dashed line). For the sake of clarity the spectra below 1.4 eV in b) and c) are plotted after multiplication by a factor of 10. The blends presented in panel a), b) and c) contain a 50% wt ratio of fullerene. d-e) Integrated PL intensity for the different recombination channels as a function of the PCBM weight ratio in the blends. For the RE-P3HT/PCBM blends only the P3HT S_1 emission is plotted. f-h) TEM pictures of ra-P3HT/PCBM, RE-P3HT/PCBM and RE-P3HT/PCBM annealed, respectively. The bright regions are representative of P3HT rich domains, while the dark ones are due to PCBM molecules. The scale bar is 100 nm.

References

[1] A. C. Morteani, A. S. Dhoot, J. S. Kim, C. Silva, N. C. Greenham, C. Murphy, E. Moons, S. Cina, J. H. Burroughes, R. H. Friend, *Adv. Mater.* **2003**, *15*, 1708.

[2] Y. R. Sun, N. C. Giebink, H. Kanno, B. W. Ma, M. E. Thompson, S. R. Forrest, *Nature (London)* **2006**, *440*, 908.

[3] C. W. Tang, *Appl. Phys. Lett.* **1986**, *48*, 183.

[4] G. Yu, J. Gao, J. C. Hummelen, F. Wudl, A. J. Heeger, *Science* **1995**, *270*, 1789.

[5] S. Morita, A. A. Zakhidov, K. Yoshino, *Solid State Commun.* **1992**, *82*, 249.

[6] Y. Kim, S. Cook, S. M. Tuladhar, S. A. Choulis, J. Nelson, J. R. Durrant, D. D. C. Bradley, M. Giles, I. McCulloch, C. S. Ha, M. Ree, *Nature Mater.* **2006**, *5*, 197.

[7] A. Haugeneder, M. Neges, C. Kallinger, W. Spirkl, U. Lemmer, J. Feldmann, U. Scherf, E. Harth, A. Gugel, K. Müllen, *Phys. Rev. B* **1999**, *59*, 15346.

[8] P. E. Shaw, A. Ruseckas, I. D. W. Samuel, *Adv. Mater.* **2008**, *20*, 3516.

[9] T. Drori, C. X. Sheng, A. Ndobe, S. Singh, J. Holt, Z. V. Vardeny, *Phys. Rev. Lett.* **2008**, *101*, 037401.

[10] J. G. Müller, J. M. Lupton, J. Feldmann, U. Lemmer, M. C. Scharber, N. S. Sariciftci, C. J. Brabec, U. Scherf, *Phys. Rev. B* **2005**, *72*, 195208.

[11] S. E. Shaheen, C. J. Brabec, N. S. Sariciftci, F. Padinger, T. Fromherz, J. C. Hummelen, *Appl. Phys. Lett.* **2001**, *78*, 841.

[12] F. Padinger, R. S. Rittberger, N. S. Sariciftci, *Adv. Funct. Mater.* **2003**, *13*, 85.

[13] M. Lenes, M. Morana, C. J. Brabec, P. W. M. Blom, *Adv. Funct. Mater.* **2009**, *19*, 1106.

[14] P. W. M. Blom, V. D. Mihailetchi, L. J. A. Koster, D. E. Markov, *Adv. Mater.* **2007**, *19*, 1551.

[15] H. Alves, A. S. Molinari, H. X. Xie, A. F. Morpurgo, *Nature Mater.* **2008**, *7*, 574.

[16] Y. S. Huang, S. Westenhoff, I. Avilov, P. Sreearunothai, J. M. Hodgkiss, C. Deleener, R. H. Friend, D. Beljonne, *Nature Mater.* **2008**, *7*, 483.

[17] J. J. Benson-Smith, L. Goris, K. Vandewal, K. Haenen, J. V. Manca, D. Vanderzande, D. D. C. Bradley, J. Nelson, *Adv. Funct. Mater.* **2007**, *17*, 451.

[18] E. F. Aziz, A. Vollmer, S. Eisebitt, W. Eberhardt, P. Pingel, D. Neher, N. Koch, *Adv. Mater.* **2007**, *19*, 3257.

[19] F. Jäckel, U. G. E. Perera, V. Iancu, K. F. Braun, N. Koch, J. P. Rabe, S. W. Hla, *Phys. Rev. Lett.* **2008**, *100*, 126102.

[20] G. Ruani, C. Fontanini, M. Murgia, C. Taliani, *J. Chem. Phys.* **2002**, *116*, 1713.

[21] J. L. Brédas, D. Beljonne, V. Coropceanu, J. Cornil, *Chem. Rev.* **2004**, *104*, 4971.

[22] Z. D. Wang, S. Mazumdar, A. Shukla, *Phys. Rev. B* **2008**, *78*.

[23] P. Parkinson, J. Lloyd-Hughes, M. B. Johnston, L. M. Herz, *Phys. Rev. B* **2008**, *78*, 115321.

[24] L. Goris, A. Poruba, L. Hod'akova, M. Vanecek, K. Haenen, M. Nesladek, P. Wagner, D. Vanderzande, L. De Schepper, J. V. Manca, *Appl. Phys. Lett.* **2006**, *88*, 052113.

[25] J. Holt, S. Singh, T. Drori, Y. Zheng, Z. V. Vardeny, *Phys. Rev. B* **2009**, *79*.

[26] A. Brillante, M. R. Philpott, *J. Chem. Phys.* **1980**, *72*, 4019.

[27] D. Veldman, O. Ipek, S. C. J. Meskers, J. Sweelssen, M. M. Koetse, S. C. Veenstra, J. M. Kroon, S. S. van Bavel, J. Loos, R. A. J. Janssen, *J. Am. Chem. Soc.* **2008**, *130*, 7721.

[28] M. Hallermann, S. Haneder, E. Da Como, *Appl. Phys. Lett.* **2008**, *93*, 053307.

[29] M. A. Loi, S. Toffanin, M. Muccini, M. Forster, U. Scherf, M. Scharber, *Adv. Funct. Mater.* **2007**, *17*, 2111.
[30] A. C. Morteani, P. Sreearunothai, L. M. Herz, R. H. Friend, C. Silva, *Phys. Rev. Lett.* **2004**, *92*, 247402.
[31] K. Vandewal, A. Gadisa, W. D. Oosterbaan, S. Bertho, F. Banishoeib, I. Van Severen, L. Lutsen, T. J. Cleij, D. Vanderzande, J. V. Manca, *Adv. Funct. Mater.* **2008**, *18*, 2064.
[32] D. Veldman, S. C. J. Meskers, R. A. J. Janssen, *Adv. Funct. Mater.* **2009**, *19*, 1939.
[33] H. Ohkita, S. Cook, Y. Astuti, W. Duffy, S. Tierney, W. Zhang, M. Heeney, I. McCulloch, J. Nelson, D. D. C. Bradley, J. R. Durrant, *J. Am. Chem. Soc.* **2008**, *130*, 3030.
[34] S. Westenhoff, I. A. Howard, J. M. Hodgkiss, K. R. Kirov, H. A. Bronstein, C. K. Williams, N. C. Greenham, R. H. Friend, *J. Am. Chem. Soc.* **2008**, *130*, 13653.
[35] J. K. J. van Duren, X. N. Yang, J. Loos, C. W. T. Bulle-Lieuwma, A. B. Sieval, J. C. Hummelen, R. A. J. Janssen, *Adv. Funct. Mater.* **2004**, *14*, 425.
[36] X. N. Yang, J. Loos, S. C. Veenstra, W. J. H. Verhees, M. M. Wienk, J. M. Kroon, M. A. J. Michels, R. A. J. Janssen, *Nano Lett* **2005**, *5*, 579.
[37] W. L. Ma, C. Y. Yang, A. J. Heeger, *Adv. Mater.* **2007**, *19*, 1387.
[38] T. Martens, J. D'Haen, T. Munters, Z. Beelen, L. Goris, J. Manca, M. D'Olieslaeger, D. Vanderzande, L. De Schepper, R. Andriessen, *Synth. Met.* **2003**, *138*, 243.
[39] H. Hoppe, M. Niggemann, C. Winder, J. Kraut, R. Hiesgen, A. Hinsch, D. Meissner, N. S. Sariciftci, *Adv. Funct. Mater.* **2004**, *14*, 1005.
[40] V. M. Burlakov, K. Kawata, H. E. Assender, G. A. D. Briggs, A. Ruseckas, I. D. W. Samuel, *Phys. Rev. B* **2005**, *72*, 075206.
[41] S. Cook, R. Katoh, A. Furube, *J. Phys. Chem. C* **2009**, *113*, 2547.
[42] J. Y. Kim, C. D. Frisbie, *J. Phys. Chem. C* **2008**, *112*, 17726.
[43] M. D. Irwin, D. B. Bucholz, A. W. Hains, R. P. H. Chang, T. J. Marks, *Proc. Natl. Acad. Sci. USA* **2008**, *105*, 2783.
[44] H. Sirringhaus, P. J. Brown, R. H. Friend, M. M. Nielsen, K. Bechgaard, B. M. W. Langeveld-Voss, A. J. H. Spiering, R. A. J. Janssen, E. W. Meijer, P. Herwig, D. M. de Leeuw, *Nature (London)* **1999**, *401*, 685.
[45] R. Österbacka, C. P. An, X. M. Jiang, Z. V. Vardeny, *Science* **2000**, *287*, 839.
[46] L. L. Chua, J. Zaumseil, J. F. Chang, E. C. W. Ou, P. K. H. Ho, H. Sirringhaus, R. H. Friend, *Nature (London)* **2005**, *434*, 194.
[47] O. J. Korovyanko, R. Osterbacka, X. M. Jiang, Z. V. Vardeny, R. A. J. Janssen, *Phys. Rev. B* **2001**, *64*, 235122.
[48] P. Yang, E. R. Batista, S. Tretiak, A. Saxena, R. L. Martin, D. L. Smith, *Phys. Rev. B* **2007**, *76*.
[49] K. Becker, E. Da Como, J. Feldmann, F. Scheliga, E. T. Csanyi, S. Tretiak, J. M. Lupton, *J. Phys. Chem. B* **2008**, *112*, 4859.
[50] S. M. Tuladhar, M. Sims, S. A. Choulis, C. B. Nielsen, W. N. George, J. H. G. Steinke, D. D. C. Bradley, J. Nelson, *Org. Elect.* **2009**, *10*, 562.
[51] J. S. Moon, J. K. Lee, S. N. Cho, J. Y. Byun, A. J. Heeger, *Nano Lett* **2009**, *9*, 230.